

# CM082 Enhances the Efficacy of Chemotherapeutic Drugs by Inhibiting the Drug Efflux Function of ABCG2

Lejia Xu,<sup>1,2,6</sup> Jiwei Huang,<sup>1,6</sup> Jie Liu,<sup>1,6</sup> Yun Xi,<sup>3,6</sup> Zongheng Zheng,<sup>4</sup> Kenneth K.W. To,<sup>5</sup> Zhen Chen,<sup>2</sup> Fang Wang,<sup>2</sup> Yongming Zhang,<sup>1</sup> and Liwu Fu<sup>2</sup>

<sup>1</sup>Department of Pharmacy, The Third Affiliated Hospital of Sun Yat-sen University, Guangzhou 510630, Guangdong, China; <sup>2</sup>State Key Laboratory of Oncology in South China, Collaborative Innovation Center for Cancer Medicine, Guangdong Esophageal Cancer Institute, Sun Yat-sen University Cancer Center, Guangzhou 510060, Guangdong, China; <sup>3</sup>Department of Clinical Laboratory, The Third Affiliated Hospital of Sun Yat-sen University, Guangzhou 510630, Guangdong, China; <sup>4</sup>Department of Gastrointestinal Surgery, The Third Affiliated Hospital of Sun Yat-sen University, Guangzhou 510630, Guangdong, China; <sup>5</sup>School of Pharmacy, The Chinese University of Hong Kong, Hong Kong, China

**The overexpression of ATP-binding cassette (ABC) transporters is one of the important mechanisms of multidrug resistance (MDR). Some tyrosine kinase inhibitors (TKIs) such as CM082 might be a potential ABC transporter inhibitor, thus potentially reversing MDR. We used a 3-(4,5-dimethylthiazol-2-yl)-2,5-dimethyltetrazolium bromide (MTT) assay to determine the cytotoxicity and reversal effect of CM082. A xenograft model was established to evaluate the reversal MDR efficacy *in vivo*. The intracellular accumulation and efflux of ABCG2 substrates were measured by flow cytometry. We investigated the binding sites of ABCG2 via photolabeling ABCG2 with [<sup>125</sup>I]-iodoarylazidoprazosin (IAAP). Quantitative real-time PCR and western blot were utilized to analyze mRNA and protein expression. We found that CM082 could enhance the efficacy of substrate in ABCG2-overexpressing cells both *in vitro* and *in vivo*. Furthermore, CM082 significantly increased intracellular accumulation of ABCG2 substrates by inhibiting the efflux activity. CM082 stimulated ABCG2 ATPase activity and competed with [<sup>125</sup>I]-IAAP photolabeling of ABCG2 in a concentration-dependent manner. However, CM082 did not alter ABCG2 expression at protein and mRNA levels or inhibit vascular endothelial growth factor (VEGF) downstream signaling of AKT and extracellular signal-regulated kinase (ERK). Further research is encouraged to confirm whether CM082 concomitant with anticancer drugs of ABCG2 substrates could improve the clinical outcomes of cancer treatment in cancer patients with ABCG2 overexpression.**

## INTRODUCTION

Multidrug resistance (MDR) limits successful cancer chemotherapy. Up to 90% of chemotherapy failures in the treatment of metastatic breast cancer and colon cancer patients were attributed to MDR.<sup>1</sup> Therefore, it has become a critical topic in the research of cancer therapy to reverse drug resistance and to improve drug sensitivity of tumor cells. The potential mechanisms of MDR include efflux pumps, apoptosis regulation, autophagy, regulation of cancer stem

cells, DNA damage and repair, and epigenetic regulation.<sup>2</sup> Among them, ATP-binding cassette (ABC) transporter overexpression has aroused great concern because it is responsible for drug efflux from tumor cells, resulting in a reduction in intracellular drug concentration and subsequent drug resistance in tumor cells.<sup>3</sup>

The family of ABC transporters is large and contains 49 members at this moment.<sup>4</sup> In particular, ABCB1, ABCG2, and ABCC1 are considered to be major contributors to MDR.<sup>5</sup> As a semi-transporter protein encoded by the *ABCG2* gene at human chromosome 4q22–23, ABCG2 is highly expressed in various kinds of cancer cells, such as breast cancer,<sup>6</sup> esophageal cancer,<sup>7</sup> nasopharyngeal cancer,<sup>8</sup> acute myeloid leukemia,<sup>9</sup> non-small-cell lung cancer,<sup>10</sup> and renal malignancy.<sup>11</sup> In addition, ABCG2 was associated with drug resistance and poor prognosis of the patients,<sup>6,11,12</sup> while the inhibition of ABCG2 expression could potentially reverse MDR.<sup>11,13</sup> Nevertheless, no drugs have been approved by the US Food and Drug Administration (FDA) as MDR modulators.

Tyrosine kinase inhibitors (TKIs) play an important role in anti-cancer treatment by blocking the binding of tyrosine kinase.<sup>14</sup> Interestingly, ABC transporters share similar ATP binding sites as those of tyrosine kinase. Increasing evidence has shown that the chemotherapeutic outcomes might be promoted by TKIs via

Received 22 August 2019; accepted 12 December 2019;  
<https://doi.org/10.1016/j.omto.2019.12.007>.

<sup>6</sup>These authors contributed equally to this work.

**Correspondence:** Yongming Zhang, PhD, Department of Pharmacy, The Third Affiliated Hospital of Sun Yat-sen University, Guangzhou 510000, Guangdong, China.

**E-mail:** 874477522@qq.com

**Correspondence:** Liwu Fu, PhD, State Key Laboratory of Oncology in South China, Collaborative Innovation Center for Cancer Medicine, Guangdong Esophageal Cancer Institute, Sun Yat-sen University Cancer Center, Guangzhou 510060, Guangdong, China.

**E-mail:** fulw@mail.sysu.edu.cn



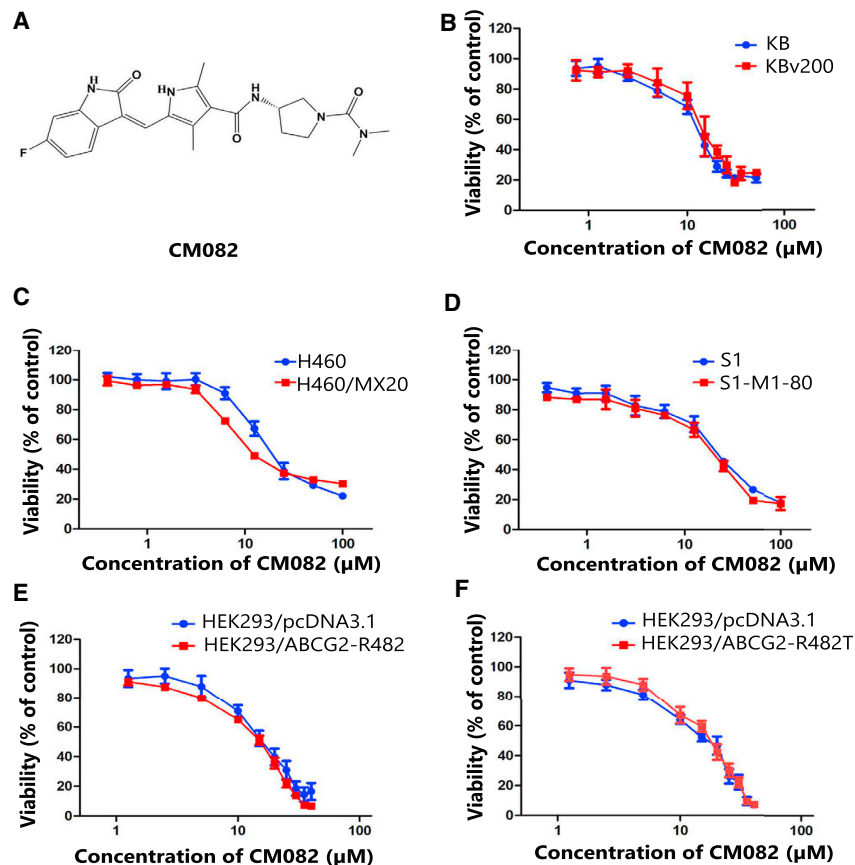


**Figure 1. Cytotoxicity of CM082 on ABCB1 and ABCG2-Overexpressing Cells and Their Parental Drug-Sensitive Cells**

(A) The structure of CM082. (B) Cytotoxicity assay of CM082 in ABCB1 overexpression KBv200 cells and their parental drug-sensitive KB cells. (C) Cytotoxicity assay of CM082 in ABCG2 overexpression H460/MX20 cells and their parental drug-sensitive H460 cells. (D) Cytotoxicity assay of CM082 in S1 and S1-MI-80 cells. (E) Cytotoxicity assay of CM082 in HEK293/pcDNA3.1 and stable transfected ABCG2-R482T (mutant) cells. (F) Cytotoxicity assay of CM082 in HEK293/pcDNA3.1 and stable transfected ABCG2-R482 (wild-type) cells. Results from three independent experiments are expressed as the mean  $\pm$  SD.

Compared to their parental cells, the 50% inhibitory concentration (IC<sub>50</sub>) of the chemotherapeutic agent in S1-MI-80, H460/MX20, and KBV200 cells was extremely high (Table 1). In S1-MI-80 and H460/MX20 cells with ABCG2 overexpression, CM082 decreased the IC<sub>50</sub> of substrate chemotherapeutic drugs such as mitoxantrone (MX) and topotecan in a concentration-dependent manner, while no notable potential effect was observed in KBV200 cells with ABCB1 overexpression (Table 1). At the same time, the IC<sub>50</sub> of cisplatin (DDP), which is not a substrate of ABCB1 or ABCG2 in both sensitive and MDR cells, was not changed by CM082. In addition, amino acid 482 mutations at ABCG2 protein were found to greatly influence

inhibiting the activity of ABC transporters.<sup>15–18</sup> As an oral TKI with multiple targets, CM082 is derived from sunitinib and can suppress angiogenesis by inactivating the pathways of platelet-derived growth factor (PDGF), vascular endothelial growth factor (VEGF), c-Kit, and Fms-like tyrosine kinase 3 (FLT3). A phase I clinical trial of CM082 has been completed in the United States to treat patients with age-related macular degeneration,<sup>19</sup> and a phase IIB trial (ClinicalTrials.gov: NCT02348359) of CM082 is underway.<sup>20</sup> In addition, a phase I trial of CM082 combined with everolimus in the treatment of metastatic renal cell carcinoma has also been carried out in China.<sup>21</sup> In this study, the role of CM082 in reversing MDR was evaluated in cancer cells with overexpressing ABCB1 and ABCG2.<sup>19</sup>

## RESULTS

### CM082 Enhanced the Sensitivity of Cells with Overexpression of ABCG2 to Chemotherapeutic Drugs *In Vitro*

To determine the concentration of CM082 in a reverse test, the cytotoxicity effects of CM082, whose structure is shown in Figure 1A, were evaluated in drug-resistant cells and their parental drug-sensitive cells via a 3-(4,5-dimethylthiazol-2-yl)-2,5-dimethyltetrazolium bromide (MTT) assay. As shown in Figures 1B–1F, more than 80% of the cells survived under the concentration of 5  $\mu$ M CM082. Thereafter, 1.25, 2.5, and 5  $\mu$ M CM082 were chosen for the reversal experiments.

the substrate specificity of ABCG2 and may reduce the effectiveness of potential ABCG2 blockers.<sup>22</sup> As shown in Table 2, the IC<sub>50</sub> of ABCG2 substrate MX in both the wild-type (R482) and mutant (R482T) cells was significantly reduced by concomitant treatment with CM082, whereas there were no alterations in the parental cells of HEK293/pcDNA3.1. These results indicated that CM082 could specifically enhance the sensitivity of a substrate chemotherapeutic agent in overexpressing ABCG2 cells, but not in overexpressing ABCB1 cells.

### CM082 Significantly Enhanced the Efficacy of Topotecan *In Vivo* of the H460/MX20 Xenograft Model

To confirm whether CM082 could also reverse MDR *in vivo*, xenograft models of nude mice were constructed by injecting H460/MX20 cells into subaxillary subcutaneously in the mice. It was found that CM082 combined with topotecan (the substrate of ABCG2) significantly inhibited xenograft growth: the inhibition rate was 68.2% ( $p < 0.001$ ), while there was no significant difference in the tumor weight and size among the control group, the topotecan group, and the CM082 group (Figures 2A–2C). These results suggested that the anti-tumor effect of topotecan on xenografts of ABCG2-overexpressing cells was enhanced by CM082. Importantly, there was no death or notable weight loss in all groups (Figure 2D), suggesting that the regimen of concomitant drug treatment did not increase toxicity.

**Table 1. Effect of CM082 on Chemotherapeutic Agents in ABC Transporter-Expressing Cells *In Vitro***

Compounds	IC <sub>50</sub> ± SD (μM) (Fold Reversal)			
	KB		KBV200	
DOX	0.0341 ± 0.0051	(1.00)	0.6153 ± 0.0678	(1.00)
+1.25 μM CM082	0.0364 ± 0.0019	(0.94)	0.6292 ± 0.0162	(0.98)
+2.5 μM CM082	0.0367 ± 0.0032	(0.93)	0.6031 ± 0.0523	(1.02)
+5 μM CM082	0.0339 ± 0.0031	(1.01)	0.6120 ± 0.0488	(1.01)
+10 μM VRP	0.0324 ± 0.0054	(1.05)	0.0983 ± 0.0067	(6.26) **
DDP	0.4626 ± 0.0668	(1.00)	2.215 ± 0.2592	(1.00)
+5 μM CM082	0.5341 ± 0.0411	(0.87)	2.3753 ± 0.0421	(0.93)
	S1		S1-MI-80	
MX	0.1669 ± 0.0205	(1.00)	3.9816 ± 0.1926	(1.00)
+1.25 μM CM082	0.1838 ± 0.0057	(0.91)	1.8476 ± 0.0819	(2.15) **
+2.5 μM CM082	0.1561 ± 0.0289	(1.07)	0.9935 ± 0.0801	(4.01) **
+5 μM CM082	0.1513 ± 0.0234	(1.10)	0.7887 ± 0.0371	(5.05) **
+2.5 μM FTC	0.1570 ± 0.0161	(1.06)	0.5602 ± 0.0806	(7.11) **
Topotecan	0.0701 ± 0.0067	(1.00)	12.593 ± 0.6403	(1.00)
+1.25 μM CM082	0.0783 ± 0.0078	(0.90)	5.264 ± 0.2486	(2.39) **
+2.5 μM CM082	0.0740 ± 0.0071	(0.95)	3.1136 ± 0.5521	(4.04) **
+5 μM CM082	0.0696 ± 0.0057	(1.01)	2.5146 ± 0.2676	(5.01) **
+2.5 μM FTC	0.0725 ± 0.0078	(0.97)	0.7126 ± 0.0874	(17.67) **
DDP	1.7123 ± 0.1378	(1.00)	3.9653 ± 0.5882	(1.00)
+5 μM CM082	1.777 ± 0.1294	(0.96)	4.1236 ± 0.4957	(0.96)
	H460		H460/MX20	
MX	0.0226 ± 0.0008	(1.00)	0.6025 ± 0.0242	(1.00)
+1.25 μM CM082	0.0234 ± 0.0020	(0.97)	0.2924 ± 0.0361	(2.06) **
+2.5 μM CM082	0.0243 ± 0.0020	(0.93)	0.2715 ± 0.0159	(2.22) **
+5 μM CM082	0.0216 ± 0.0022	(1.04)	0.147 ± 0.0167	(4.10) **
+2.5 μM FTC	0.0216 ± 0.0013	(1.04)	0.0928 ± 0.0047	(6.49) **
DDP	2.4503 ± 0.4176	(1.00)	6.5106 ± 0.3045	(1.00)
+5 μM CM082	2.9673 ± 0.3366	(0.83)	6.268 ± 0.1615	(0.96)

An MTT assay was carried out to evaluate cell survival. VRP and FTC were employed as ABCB1- and ABCG2-positive control inhibitors, respectively. IC<sub>50</sub> values are shown as mean ± SD based on three separate experiments. By dividing the IC<sub>50</sub> of cells free from CM082 with the IC<sub>50</sub> of cells under CM082, we obtained the fold reversal of MDR. \*\*p < 0.01.

### CM082 Enhances the Accumulation of Substrates in ABCG2-Mediated MDR Cells

The results from the cytotoxicity assay and xenograft model in mice showed that the sensitivity of MDR tumor cells to ABCG2 substrates was improved by CM082. For exploration of the possible mechanisms, the accumulation of Hoechst 33342, rhodamine 123 (Rho 123), or doxorubicin (DOX) was examined by flow cytometry in the absence or presence of CM082 in ABCG2-mediated MDR cells and their parental sensitive cells. It was shown that the accumulation of ABCG2 substrate in MDR cells was significantly less compared to the parental cells (Figures 3A–3C). With CM082, the DOX accumu-

lation in S1-MI-80 cells was increased significantly in a concentration-dependent manner, while their parental sensitive S1 cells showed no difference in terms of DOX accumulation (Figure 3B). The action of 5 μM CM082 was comparable to that of fumitremorgin C (FTC), with 2.5 μM as the positive control agent (Figure 3B). These results indicated that the accumulation of ABCG2 substrates in overexpression of ABCG2 cells was increased by CM082.

ABC transporter-mediated MDR is mainly caused by chemotherapeutic drug efflux from tumor cells, hence decreasing their accumulation in the cells. Therefore, a drug efflux assay was further conducted in this study to determine whether CM082 inhibited the outflow of ABCG2 substrates. In S1-MI-80 cells that overexpressed ABCG2, Rho 123 efflux was significantly higher compared to that of S1 cells. With CM082, efflux ratios of Rho 123 were decreased at all time points (Figure 4A). In addition, CM082 showed no effect on its efflux in S1 cells. These results suggested that CM082 inhibited ABCG2 efflux activity.

### CM082 Inhibited the [<sup>125</sup>I]-IAAP Photoaffinity Labeling of ABCG2

[<sup>125</sup>I]-iodoarylazidoprazosin (IAAP) labeling is widely used to determine the binding region between ABCG2 and its substrates or inhibitors.<sup>23</sup> In order to determine the competitive site between CM082 and ABCG2 substrates, membrane vesicles were incubated at different concentrations of CM082, followed by detection of the ABCG2 photolabeling effect of [<sup>125</sup>I]-IAAP. As shown in Figure 4B, CM082 exerted an obvious inhibitory effect on [<sup>125</sup>I]-IAAP photoaffinity labeling of ABCG2. The facts above indicated that CM082 might compete with the ABCG2 substrate for protein binding sites, thereby inhibiting the pump out of ABCG2 substrates.

### ABCG2 ATPase Activity Was Stimulated by CM082

Under substrates, ATP hydrolysis will be activated, and drugs are pumped out of cells by ABC transporters. Therefore, ATP consumption reflects ATPase activity. In this study, we detected ATPase activity of ABCG2 (vanadium-sensitive) at various concentrations of CM082 to ascertain CM082's role in ATPase activity. As shown in Figure 4C, the ATPase activity of ABCG2 was promoted by CM082 until the plateau, which was close to 76 nmol/min/mg of protein, was achieved. It seems that, similar to other substrates of ABCG2, ATPase activity was stimulated by CM082 through binding to the sites at transporters. The results suggested that CM082 might be a substrate of ABCG2.

### Cell Surface Localization and Expressions of ABCG2 Were Not Changed by CM082

In addition to inhibiting the efflux pump function, ABCG2 reversal may be achieved by reducing its expression. In this study, ABCG2 mRNA and protein expressions were measured using quantitative real-time PCR and western blot after incubation of the cells with various concentrations of CM082. Meanwhile, the expression of ABCG2 on the surface of ABCG2-overexpressing cells was analyzed using flow cytometry. Even at the highest concentration, CM082 did not influence the protein expression of ABCG2 and its membrane location (Figures 5A–5C). It seems that the mRNA level was increased

**Table 2. Effect of CM082 on Chemotherapeutic Agents in ABCG2 Wild and Mutation Stably Transfected Cells**

Compounds	IC <sub>50</sub> ± SD (μM) (Fold Reversal)					
	HEK293/pcDNA3.1		HEK293-R482 (Wild)		HEK293-R482T (Mutation)	
MX	0.0105 ± 0.0010	(1.00)	0.1287 ± 0.0103	(1.00)	0.1752 ± 0.0091	(1.00)
+1.25 μM CM082	0.0098 ± 0.0008	(1.07)	0.0752 ± 0.0074	(1.71)**	0.1005 ± 0.0040	(1.74)**
+2.5 μM CM082	0.0103 ± 0.0008	(1.02)	0.0221 ± 0.0025	(5.80)**	0.0846 ± 0.0014	(2.07)**
+5 μM CM082	0.0088 ± 0.0002	(1.19)	0.0155 ± 0.0030	(8.29)**	0.0581 ± 0.0027	(3.02)**
+2.5 μM FTC	0.0094 ± 0.0004	(1.11)	0.0123 ± 0.0017	(10.41)**	0.0253 ± 0.0027	(6.90)**
DDP	4.459 ± 0.2491	(1.00)	2.592 ± 0.3561	(1.00)	0.7877 ± 0.0312	(1.00)
+5 μM CM082	4.8846 ± 0.1330	(0.91)	2.5063 ± 0.3948	(1.03)	0.8464 ± 0.1042	(0.93)

An MTT assay was carried out to evaluate cell survival. FTC was set as positive MDR modulator controls. IC<sub>50</sub> values are shown as mean ± SD based on three separate experiments. By dividing the IC<sub>50</sub> of cells free from CM082 with the IC<sub>50</sub> of cells under CM082, we obtained the fold reversal of MDR. \*\* p < 0.01.

1.3- to 1.5-fold after incubation of the CM082 (Figure 5D), but this difference was not statistically significant ( $p > 0.2$ ). These results suggested that the reversal of MDR by CM082 was not associated with the alteration of ABCG2 expression in protein and mRNA levels and its membrane location.

#### Phosphorylation of ERK and AKT at Concentrations of MDR Reversal Was Not Blocked by CM082

It was reported that extracellular signal-regulated kinase (ERK) and AKT pathway suppression might improve outcomes of chemotherapeutic drugs in cancer cells.<sup>24,25</sup> As a potent inhibitor of VEGF receptor (VEGFR) and PDGF receptor (PDGFR), CM082 could regulate the activation of AKT and ERK, two important downstream factors of the ERK and AKT pathways. In this study, the phosphorylation of AKT and ERK was tested over a range of different concentrations using western blot. The phosphorylation and general levels of ERK and AKT in ABCG2 overexpression S1-MI-80 cells and H460/MX20 cells were not changed by CM082 (Figure 6). These results suggested that the reversal of MDR by CM082 did not involve the blockage of AKT or ERK phosphorylation.

#### DISCUSSION

Since ABC transporters have been identified as an important contributor to MDR, many studies have focused on the modulators of ABC transporters. During the past 30 years, four distinct generations of inhibitors have been developed to target ABC transporters. However, due to the toxicity of these inhibitors and their interaction with chemotherapeutic agents, no such inhibitors have been approved for clinical use. Recently, increasing evidence has shown that TKIs can reverse MDR mediated by ABC transporters.<sup>26</sup> In some clinical trials, concomitant use of TKIs might be beneficial for patients who showed no response to chemotherapeutic drugs due to drug resistance.

As a derivative of sunitinib, CM082 is a multilocus TKI that can be administered orally. Because of its short half-life and low tissue accumulation, CM082 has better tolerance than that of similar drugs. Phase I and II clinical trials of CM082 in combination with everolimus to treat metastatic renal cell tumors are currently underway. Previous studies have shown that sunitinib can inhibit ABCG2.<sup>15</sup> In

this study, the ability of CM082 to reverse MDR was first explored *in vitro* and *in vivo*.

The results of this study showed that KB cells and KBV200 cells, S1 cells and S1-MI-80 cells, H460 cells and H460/MX20 cells, and HEK293/pcDNA3.1 cells and stable transfection HEK293/ABCG2-R482 (wild) cells, as well as HEK293/ABCG2-R482T (mutation) cells, displayed similar sensitivity to CM082. The overexpression of functional ABCB1 or ABCG2 rendered no obvious resistance to CM082. Alternatively, H460/MX20 cells and S1-MI-80 cells were extremely resistant to substrate chemotherapeutic agents such as topotecan and MX (Table 1). Co-incubation with more than 80% cell survival concentration of CM082 significantly reversed resistance to topotecan or MX in H460/MX20 and S1-MI-80 cells, but it showed no such effects in parental cells (Table 1). In addition, CM082 exerted no obvious effect of reversal on ABCB1-mediated MDR in KBv200 cells. Furthermore, to confirm the effect of CM082 on reversal of ABCG2-mediated MDR *in vivo*, the models of H460/MX20 cell xenografts were established in nude mice, and then we assessed the reversal of MDR by CM082 *in vivo*. The results showed that neither topotecan alone nor CM082 alone inhibited xenograft growth; however, the combination of CM082 and topotecan significantly inhibited xenograft growth, and the inhibition rate was 68.2%. These findings suggest that CM082 could enhance the efficacy of substrate chemotherapeutic agents *in vitro* and *in vivo*. Importantly, no animal death and weight loss were observed in topotecan alone or CM082 alone, but also in the combination of topotecan and CM082. These results demonstrate that the combination of topotecan and CM082 did not increase the toxicity or that the toxicity is endurable. These results encourage further study on combination therapy of CM082 and chemotherapeutic drugs in the clinic for cancer patients with ABCG2 overexpression. To further explore the mechanisms underlying the reversal of drug resistance mediated by ABCG2, the function or expression of ABCG2 was investigated in the absence or presence of CM082. The results showed that CM082 inhibited the efflux of substrate, such as Hoechst 33342, DOX, and Rho 123, from ABCG2-overexpressing cells, thereby increasing their intracellular accumulation. Furthermore, ABC transporters use ATP enzyme to hydrolyze the energy released by ATP to pump the substrate out of the cells. Thus, ATP hydrolysis rates are in

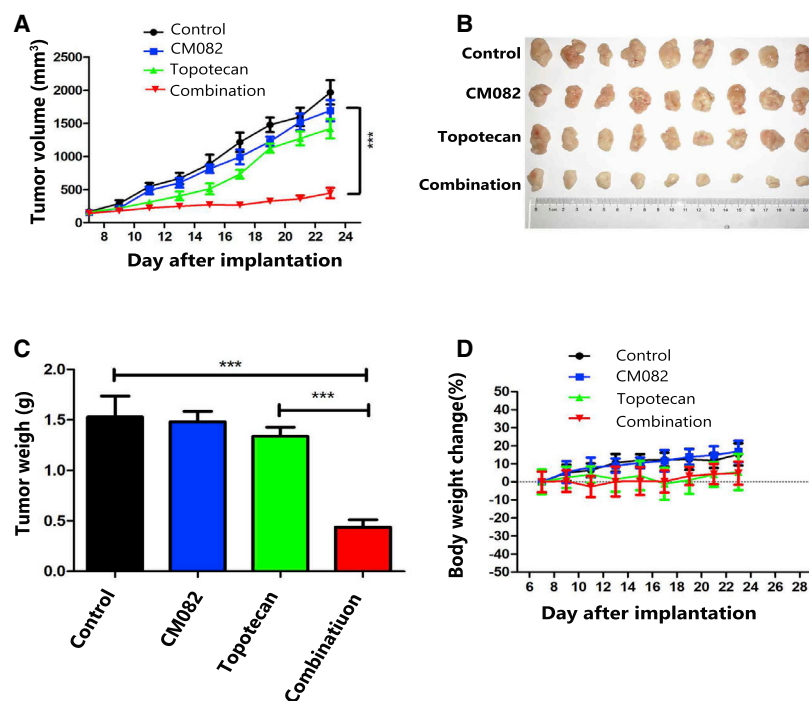


**Figure 2. CM082 Significantly Enhanced the Efficacy of Topotecan in the Model of H460/MX20 Cell Xenograft in Nude Mice**

(A) The tumor growth curve after implantation in each group ( $n = 10$ ). (B) The tumor masses were resected on day 23 after implantation and tumor sizes were exhibited. (C) Average tumor weight at the end of the experiment. The four treatment groups were as follows: control, CM082 alone, topotecan alone, and CM082 plus topotecan. (D) Body weight changes were measured once every 2 days. Results are presented as the mean  $\pm$  SD. \*\*\* $p < 0.001$ .

line with the activity of transporters. It was found in this study that the ATPase activity of ABCG2 was enhanced by CM082 at the concentrations of reversal MDR, suggesting that CM082 might be a substrate of ABCG2. The results of competition experiments on [<sup>125</sup>I]-IAAP affinity labeling also confirmed the above hypothesis. These findings suggested that CM082 might compete with substrates and incorporate into the substrate-binding sites of ABCG2. Consistent with our previous findings on other TKIs,<sup>19,26,27</sup> CM082 could antagonize the function of ABCG2. Subsequently, the effect of CM082 on ABCG2 expression was measured. It was found that ABCG2 transporter mRNA and protein levels were not changed by CM082, and their membrane location was not altered. In addition, the phosphorylation of ERK and AKT was not influenced by 5  $\mu$ M CM082 in MDR cells and their parental sensitive cells. Therefore, the MDR reversal by CM082 did not involve blockage of the ERK and AKT pathways.

In conclusion, CM082 increased the accumulation of ABCG2 substrates in ABCG2 overexpression cells by competitively suppressing ABCG2 activity (Figure 7), rather than by downregulating ABCG2 expressions or by blocking the phosphorylation of downstream effectors of VEGFR. Therefore, further study is needed to determine whether CM082 can be used concomitantly with known anticancer drugs of ABCG2 substrates to improve the clinical outcomes of cancer patients with ABCG2 overexpression.

## MATERIALS AND METHODS

### Main Reagents

CM082 was provided from Kanaji (Shanghai, China). Rho 123, MX, topotecan, DOX, DDP, FTC, Hoechst 33342, MTT, DMSO

(dimethyl sulfoxide), and VRP (verapamil) were purchased from Sigma-Aldrich (St. Louis, MO, USA). FBS (fetal bovine serum), RPMI 1640, and DMEM (Dulbecco's modified Eagle's medium) were obtained from Gibco-BRL (Gaithersburg, MD, USA). Antibodies against phosphorylated (phospho-)AKT, phospho-ERK, ABCG2, total AKT, and total ERK were provided by Santa Cruz Biotechnology (Paso Robles, CA, USA). The antibody against GAPDH was provided by Kangcheng (Shanghai, People's Republic of China). ExCell Bio (Shanghai, People's Republic of China) provided SYBR Green qPCR master mix.

### Culture of Cell Lines

Cell lines employed included the following: cell line KB (human oral epidermoid carcinoma) and cell line KBv200, which were selective for vincristine (VCR) and overexpressed ABCB1; an NSCLC cell line H460 and cell line H460/MX20, which were selective for MX and overexpressed ABCG2; cell line S1 (human colon carcinoma) and cell line S1-MI-80, which were selected for MX and overexpressed ABCG2; and a HEK293/ABCG2-R482T cell line (mutant), a HEK293/ABCG2-R482 cell line (wild-type), as well as a HEK293/pcDNA3.1 cell line were stably transfected human embryonic kidney cell lines, which were donated by Dr. Susan Bates (NCI, NIH, Bethesda, MD, USA). All cells were cultured at 37°C in a humidified incubator containing 5% CO<sub>2</sub> and RPMI 1640 or DMEM supplemented with FBS (10%). All cells were kept free from drugs for more than 2 weeks before the experiment. The transfected cells were subjected to culture with a medium that contained 2 mg/mL G418.

### Cell Cytotoxicity Assay

In order to evaluate *in vitro* drug cytotoxicity, the MTT assay was performed according to previous literature.<sup>28</sup> In brief, the cells (3,000–5,000 cells or so) of logarithmic phase were placed in 96-well microplates for 24 h of incubation, and then treated with conventional chemotherapeutic drugs in a range of different concentrations for 72 h. For the reversal experiments, the cells were preincubated with a fixed concentration of CM082, VRP, or

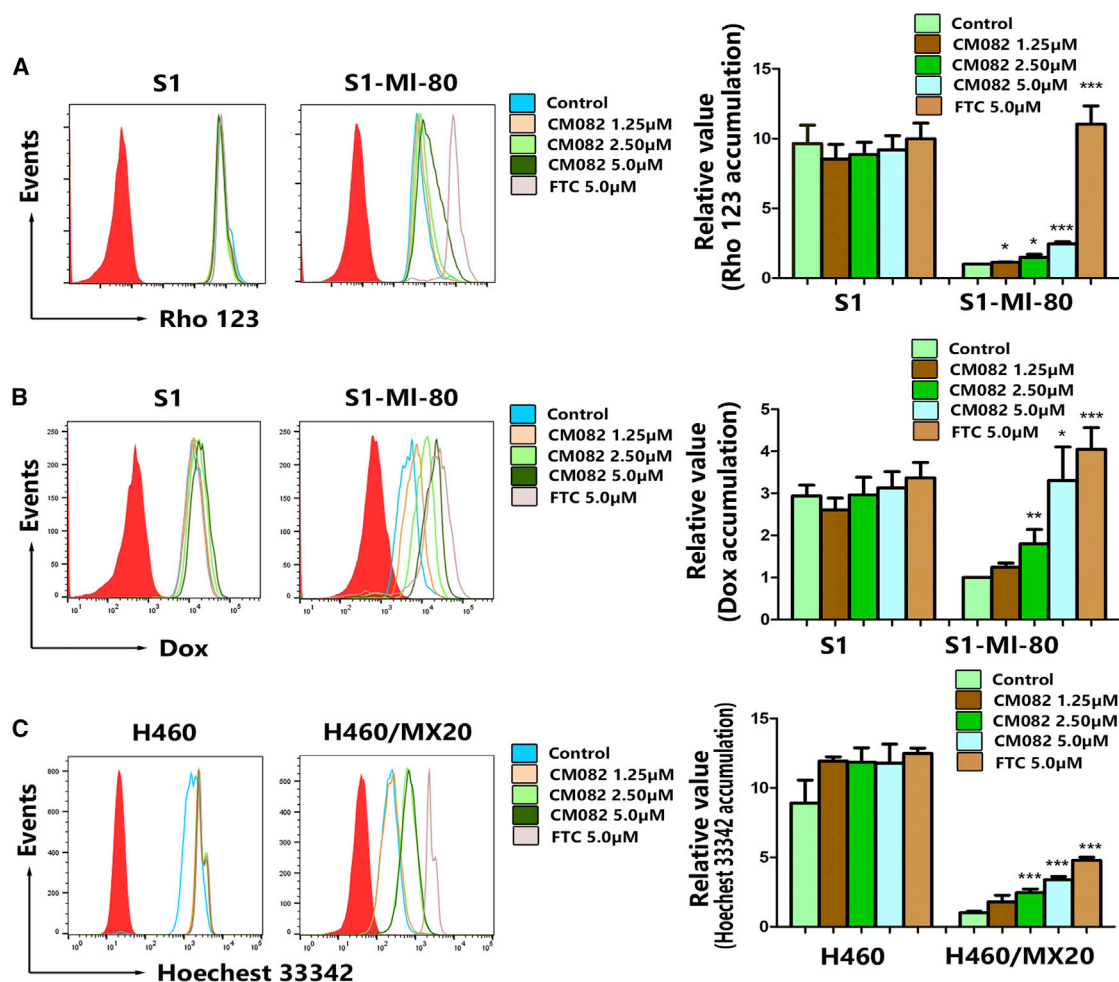


**Figure 3. CM082 Increased Intracellular Accumulation of ABCG2 Substrate in HX460/MX20 and S1-MI-80 cells**

(A) The accumulation of Rho 123 in S1 and S1-MI-80 in the absence and presence of CM082. (B) The accumulation of DOX in S1 and S1-MI-80 in the absence and presence of CM082. (C) The accumulation of Hoechst 33342 in HX460 and HX460/MX20 in the absence and presence of CM082. Fold changes in fluorescence intensity relative to controls were used to describe the data. The bars represented the mean and standard deviation. \* $p < 0.05$ , \*\* $p < 0.01$ , \*\*\* $p < 0.001$

FTC. Into each well the MTT (20  $\mu$ L, 5 mg/mL) was added following a 4-h incubation, and centrifugation was performed. The medium was discarded. Subsequently, 150  $\mu$ L of DMSO was added into each well for dissolution of formazan crystals. The absorbance was measured at a wavelength of 540 nm on a model 550 microplate reader (Bio-Rad, Hercules, CA, USA). The Bliss method was employed to calculate  $IC_{50}$ .<sup>29</sup> Through dividing the  $IC_{50}$  of cells free from CM082 with the  $IC_{50}$  of cells in the presence of CM082, we obtained the fold reversal of MDR.<sup>30</sup> All assays were performed in triplicate, and mean  $\pm$  standard deviation (SD) was used to describe the related data.

#### Animal Experiments

Based on a previous report,<sup>31</sup> H460/MX20 cell xenograft models were constructed. Briefly, H460/MX20 cells ( $3 \times 10^6$ ) from Sun Yat-sen University (Guangzhou, China) were subcutaneously injected into

the right flank of female athymic nude mice (BALB/c-nu/nu) aged 5–6 weeks and weighing 15–17 g. When the mean diameter of xenograft tumors reached 5 mm, the animals were randomly divided into four groups to receive alternative treatments: (1) control (normal saline, gavage, once every 2 days); (2) CM082 (20 mg/kg, gavage, once every 2 days); (3) topotecan (2 mg/kg, intraperitoneal injection, once every 2 days); and (4) CM082 (20 mg/kg, gavage, once every 2 days, given 1 h before the administration of topotecan) plus topotecan (2 mg/kg, intraperitoneal injection, once every 2 days). The two perpendicular diameters (length and width) of the tumor and the body weight were recorded once every 2 days. Based on the formula of tumor volume =  $(\pi/6)[(\text{length} + \text{width})/2]^3$ , tumor volume was calculated. The mice were finally euthanized, and the xenograft tumors were harvested from the mice and the weight was recorded. The ratio of growth inhibition (IR) was calculated according to the following equation:

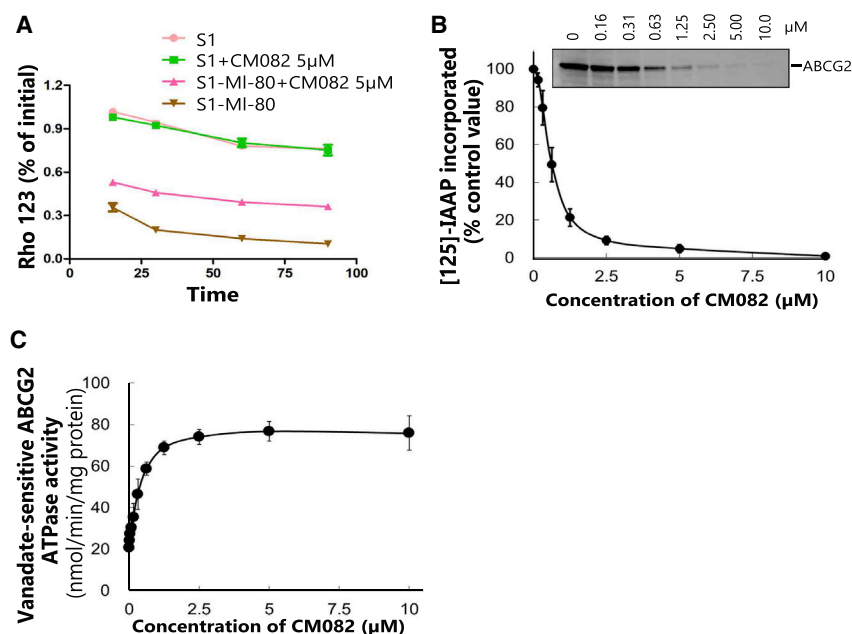


**Figure 4. The Inhibition of [<sup>125</sup>I]-IAAP Photoaffinity Labeling, the Stimulation of ATPase Activity of ABCG2, and the Decrease of Rho 123 Efflux Were Induced by CM082**

(A) In course of time, the change of Rho 123 efflux was determined in S1-MI-80 cells and S1 cells with 5 µM CM082 or not. (B) The ATPase activity of vanadate-sensitive ABCG2 under the indicated concentrations of CM082 was assessed. (C) The relative amount of [<sup>125</sup>I]-IAAP that was incorporated to the ABCG2 protein was plotted against the concentration of CM082 used in the competition. 100% incorporation indicated that CM082 was vacant. The mean and standard error values are shown.

#### Determination of ABCG2 ATPase Activity

ATPase activity of ABCG2, which was sensitive to vanadate, was detected according to a previous method with some modifications.<sup>32</sup> In detail, crude membranes were separated from MCF7/FLV1000 cells (ABCG2 overexpressing, 100 µg of protein/mL) and underwent incubation of CM082 with various concentrations with and without sodium orthovanadate (1.2 mM) in a buffer solution (1 mM DTT,

5 mM sodium azide, 50 mM KCl, 10 mM MgCl<sub>2</sub>, and 2 mM EDTA; pH 6.8) at 37°C for 5 min. For ATP hydrolysis reaction, 5 mM Mg-ATP (60 µL) was added, followed by incubation at 37°C for 10 min. The reaction was then stopped by adding 30 µL of 10% SDS. Finally, the reagent (10% ascorbic acid, 15 mM zinc acetate, and 35 mM ammonium molybdate) was added and allowed to incubate at 37°C for 20 min. The absorbance of the resulting solution was finally detected at a wavelength of 750 nm. The calibration curve was used to quantify the released inorganic phosphate. The discrepancy between the amounts of released inorganic phosphate with and without sodium orthovanadate was calculated based on vanadate-sensitive and CM082-stimulated ABCG2 ATPase activity.

#### [<sup>125</sup>I]-IAAP Was Used to Label Photoaffinity of ABCG2 and ABCB1

The crude membrane (50 µg of protein) was separated from MCF7/FLV1000 cells, and 0–10 µM CM082 was added in 50 mM Tris-HCl (pH 7.5) for a 5-min incubation at room temperature. With protection from light, [<sup>125</sup>I]-IAAP (3 nM; 2,200 Ci/nmol) was added for another 5-min incubation. Radioactive IAAP could cross-link with the ABCG2 protein by ultraviolet illumination (at a wavelength of 365 nm). Specific ABCG2 monoclonal antibody (BXP21) was introduced for immunoprecipitation of the labeled ABCG2. The samples were added to 7% Tris-acetate NuPAGE gel for sodium dodecyl sulfate polyacrylamide gel electrophoresis. After that, they were dried, followed by exposure to Bio-Max MR film (Eastman Kodak, USA) for one night at –8°C. The Storm 860 phosphorimager system (Molecular Dynamics, Sunnyvale, CA, USA) was introduced for radioactivity determination.

The ratio of growth inhibition = 1

$$\frac{\text{Averaged tumor weight in experiment group}}{\text{Averaged tumor weight in control group}} \times 100.$$

All mice were allowed free access to disinfected water and food. The protocol obtained approval from the Institutional Animal Care and Use Committee of Sun Yat-sen University Cancer Center (L102042018080C).

#### Determination of Substrate Accumulation in the Cells

Flow cytometry was employed to determine Hoechst 33342, Rho 123, and DOX in HX460/HX460/MX20 and S1/S1-MI-80 cells based on a previous report with minor changes.<sup>27</sup> In brief, the cells were cultured in six-well plates, which were then incubated for one night before treatment. Subsequently, 1.25, 2.5, or 5 µM CM082 (or vehicle and 2.5 µM FTC) was added into the medium, respectively, and the cells were further incubated at 37°C for 3 h. In the next step, 1 µM Hoechst 33342, 10 µM DOX, or 5 µM Rho 123 was added onto the cells, which were incubated for either 30 min or 3 h, respectively. Finally, the cells were harvested, followed by washing with PBS (ice-cold) three times and resuspension in 200 µL of PBS.

#### Determination of Rho 123 Efflux

Based on the previous literature,<sup>27</sup> a Rho 123 efflux assay was carried out. Rho 123 (5 µM) was added into S1-MI-80 and S1 cells for treatment for 30 min at 37°C. Subsequently, the cells were incubated with fresh media with and without 5 µM CM082 at 37°C after PBS washing for three times. The cells were then harvested at 0, 15, 30, 60, and 90 min of incubation, respectively, followed by PBS (ice-cold) washing for three times and resuspension with 200 µL of PBS for subsequent analysis.

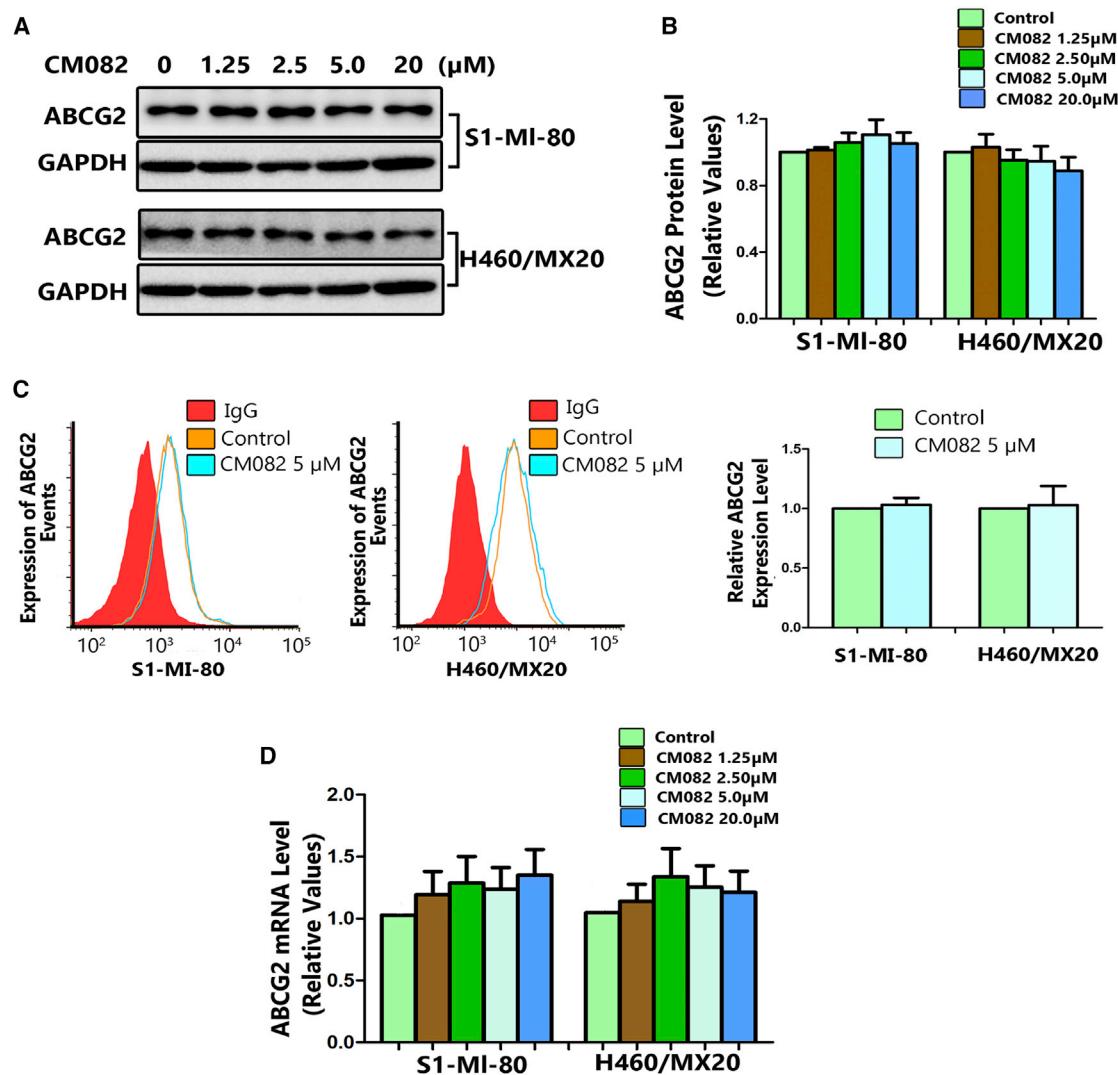


**Figure 5. CM082 Did Not Alter the Expression of ABCG2 in mRNA or Protein Levels**

After incubation with various concentrations of CM082 for 48 h, the protein levels of ABCG2 in MDR cells were measured by Western blot analysis (A) and then quantitative analysis (B). (C) Flow cytometry was used to detect ABCG2 expressions on the cell surface in H460/MX20 cells and S1-MI-80 cells, as well as in their parental drug-sensitive cells with/without CM082. (D) Real time-PCR was used to detect ABCG2 mRNA levels. All experiments were done in triplicate at least. The bars represent the mean and standard deviation.

#### Determination of ABCG2 Expressions on Cell Surface

The cellular localization of ABCG2 was determined based on a previous method.<sup>27</sup> Briefly, S1-MI-80 and H460/MX20 cells that over-expressed ABCG2 were collected and treated by 5  $\mu\text{M}$  CM082 for 45 min at 4°C after PBS washing for three times. Fluorescein isothiocyanate (FITC)-conjugated ABCG2 was used as the positive control, while FITC-labeled murine IgG2b (immunoglobulin G2b) was used as the negative control. Finally, after PBS buffer (containing 0.5% BSA) washing twice, the cells were resuspended in PBS buffer (200  $\mu\text{L}$ ).

#### Western Blot

The protein expressions were detected by western blot according to a previous method.<sup>33</sup> After treatment of S1-MI-80 and H460/MX20

cells with different concentrations of CM082 for 48 h, ABCG2 protein expressions were detected. At the same time, to explore the effect of CM082 on the downstream signaling pathway in the concentration of reversal MDR, the protein expression of AKT and ERK as well as their level of phosphorylation in S1-MI-80 cells and H460/MX20 cells and their parental cells were detected.

The prepared cell lysates were quantified by Pierce™ BCA Protein Assay Kit (Thermo Scientific, USA) according to the manuals. Protein samples were subjected to SDS-PAGE and then blotted to nitrocellulose membranes. After being blocked by 5% skim milk, membranes were subsequently incubated with the primary antibodies for one night at 4°C before incubation with corresponding secondary antibodies.



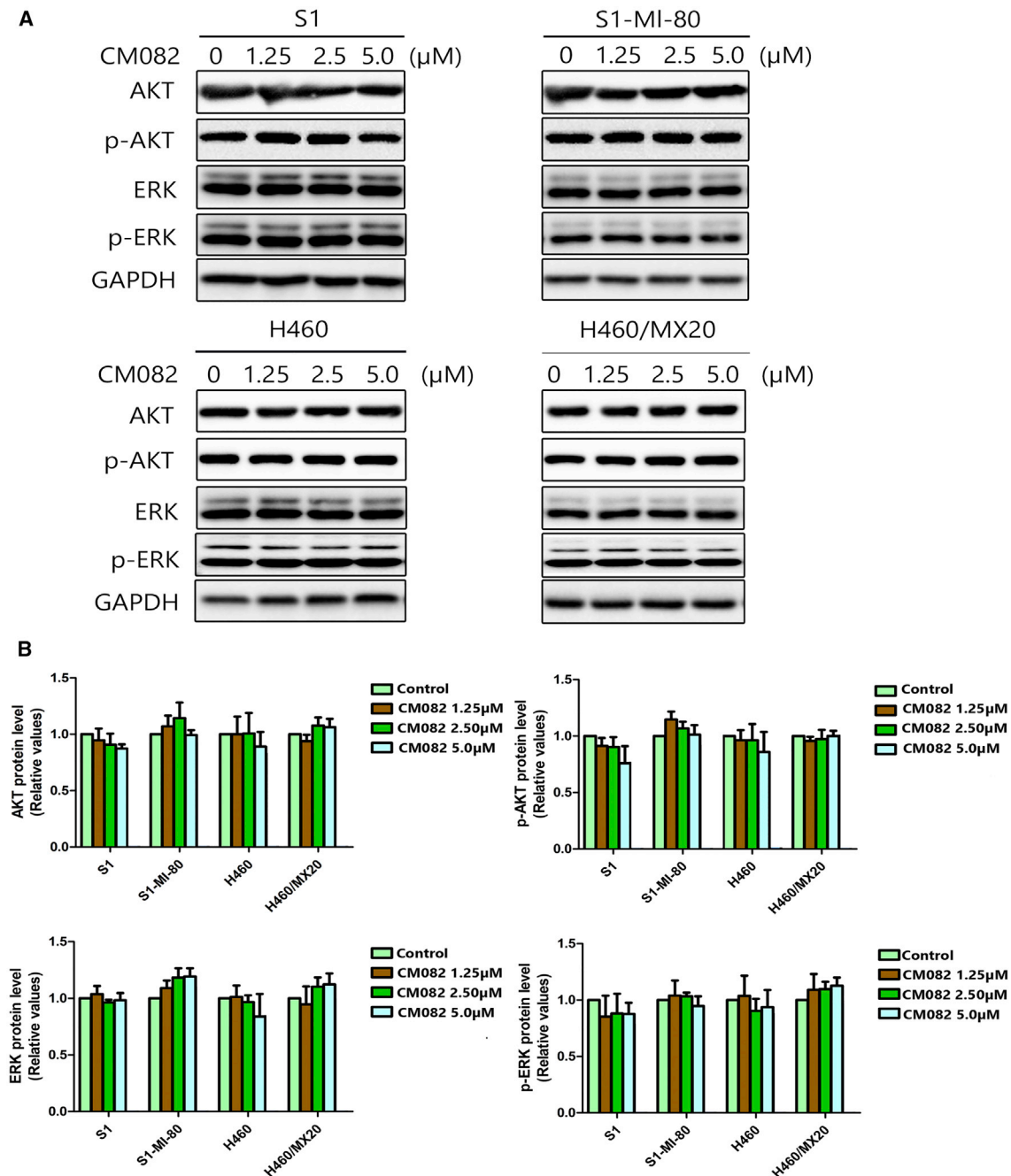


**Figure 6. CM082 Did Not Affect the Phosphorylation and General Levels of ERK and AKT**

The GAPDH was performed as loading control. (A) The total and the phosphorylation protein level of AKT and ERK were detected by western blot. (B) Quantitative analysis of AKT, ERK, and their phosphorylation. All experiments were done in triplicate at least. The bars represent mean and standard deviation.

The immunoblots were detected using an Odyssey infrared imaging system (provided by LI-COR Biosciences).

#### Quantitative Real-Time PCR

Using the previous method,<sup>34</sup> ABCG2 mRNA expression levels were determined. Various concentrations of CM082 were added for treatment

of S1-MI-80 and H460/MX20 cells for 48 h, and a TRIzol reagent RNA extraction kit (Molecular Research Center, USA) was employed to harvest total cellular RNA from each sample. PCR primers were as follows: GAPDH, forward, 5'-CTTTGGTATCGTGAAGGA-3', reverse, 5'-CACCTGTGCTGTAGCC-3'; ABCG2, forward, 5'-TGGCTGT CATGGCTTCAGTA-3', reverse, 5'-GCCACGTGATTCTTCCACA

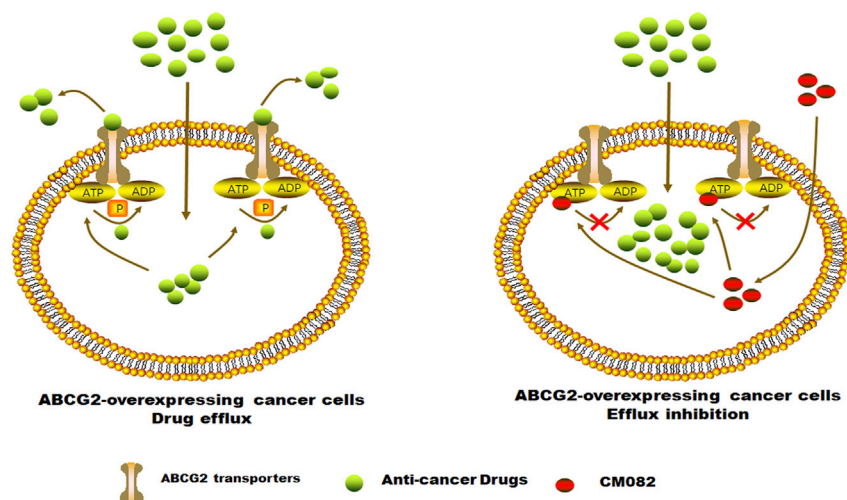


**Figure 7. A Schematic Model Illustrating the Reversal of MDR by CM082**

Overexpression of ABCG2 in MDR cancer cells leads to the efflux of antitumor drugs. CM082 could inhibit ABCG2 pump. In consequence, the accumulation of anticancer drugs in tumor cells increased, resulting in sensitivity to antitumor drugs.

A-3'. The  $2^{-\Delta\Delta Ct}$  method was employed to quantify relative expressions of ABCG2, and GAPDH expressions were used as the internal control.<sup>35</sup>

#### Statistical Analysis

GraphPad Prism 5.0 software was employed for statistical analysis. Mean  $\pm$  SD was used to describe the related data. Means between two groups were compared by Student's t test, and  $p < 0.05$  indicated significant difference.

#### Availability of Data and Materials

The authenticity of this article has been validated by uploading the key raw data onto the Research Data Deposit public platform ([www.researchdata.org.cn](http://www.researchdata.org.cn)), with the approval RDD number as RDDB2019000787.

#### AUTHOR CONTRIBUTIONS

L.X., J.H., J.L., and Y.X. were involved in study concept and design, acquisition of data, analysis and interpretation of data, and drafting of the manuscript. Z.Z., K.K.W.T., Z.C., and F.W. performed statistical analysis and conducted experiments. Y.Z. and L.F. provided material support and study supervision. All authors read and approved the final manuscript.

#### CONFLICTS OF INTEREST

The authors declare no competing interests.

#### ACKNOWLEDGMENTS

This work was supported by grants from the National Science and Technology Major Project "Key New Drug Creation and Manufacturing Program" of China (No. 2018ZX09711002-003-011) and Guangzhou Development District Leading Talents Program (No. CY2018-002).

The authors thank Dr. Susan Bates (Columbia University/New York Presbyterian Hospital, Manhattan, NY, USA) for the ABCG2-overexpressing cell lines.

#### REFERENCES

- Moulder, S. (2010). Intrinsic resistance to chemotherapy in breast cancer. *Womens Health (Lond)* 6, 821–830.
- Wu, Q., Yang, Z., Nie, Y., Shi, Y., and Fan, D. (2014). Multi-drug resistance in cancer chemotherapeutics: mechanisms and lab approaches. *Cancer Lett.* 347, 159–166.
- Gillet, J.P., Efferth, T., and Remacle, J. (2007). Chemotherapy-induced resistance by ATP-binding cassette transporter genes. *Biochim. Biophys. Acta* 1775, 237–262.
- Dean, M., Rzhetsky, A., and Allikmets, R. (2001). The human ATP-binding cassette (ABC) transporter superfamily. *Genome Res.* 11, 1156–1166.
- Lage, H. (2003). ABC-transporters: implications on drug resistance from microorganisms to human cancers. *Int. J. Antimicrob. Agents* 22, 188–199.
- Yoh, K., Ishii, G., Yokose, T., Minegishi, Y., Tsuta, K., Goto, K., Nishiwaki, Y., Kodama, T., Suga, M., and Ochiai, A. (2004). Breast cancer resistance protein impacts clinical outcome in platinum-based chemotherapy for advanced non-small cell lung cancer. *Clin. Cancer Res.* 10, 1691–1697.
- Liu, L., Zuo, L.F., and Guo, J.W. (2014). ABCG2 gene amplification and expression in esophageal cancer cells with acquired adriamycin resistance. *Mol. Med. Rep.* 9, 1299–1304.
- Huang, Y., Wang, Y., Li, Y., Guo, K., and He, Y. (2011). Role of sorafenib and sunitinib in the induction of expressions of NKG2D ligands in nasopharyngeal carcinoma with high expression of ABCG2. *J. Cancer Res. Clin. Oncol.* 137, 829–837.
- Damiani, D., Tiribelli, M., Geromin, A., Cerno, M., Zanini, F., Michelutti, A., and Fanin, R. (2016). ABCG2, cytogenetics, and age predict relapse after allogeneic stem cell transplantation for acute myeloid leukemia in complete remission. *Biol. Blood Marrow Transplant.* 22, 1621–1626.
- Kim, S.H., Kim, M.J., Cho, Y.J., Jeong, Y.Y., Kim, H.C., Lee, J.D., Hwang, Y.S., Kim, I.S., Lee, S., Oh, S.Y., et al. (2015). Clinical significance of ABCG2 haplotype-tagging single nucleotide polymorphisms in patients with unresectable non-small cell lung cancer treated with first-line platinum-based chemotherapy. *Am. J. Clin. Oncol.* 38, 294–299.
- Sato, H., Siddig, S., Uzu, M., Suzuki, S., Nomura, Y., Kashiba, T., Gushimiyagi, K., Sekine, Y., Uehara, T., Arano, Y., et al. (2015). Elacridar enhances the cytotoxic effects of sunitinib and prevents multidrug resistance in renal carcinoma cells. *Eur. J. Pharmacol.* 746, 258–266.

12. Calcagno, A.M., Fostel, J.M., To, K.K., Salcido, C.D., Martin, S.E., Chewning, K.J., Wu, C.P., Varticovski, L., Bates, S.E., Caplen, N.J., and Ambudkar, S.V. (2008). Single-step doxorubicin-selected cancer cells overexpress the ABCG2 drug transporter through epigenetic changes. *Br. J. Cancer* 98, 1515–1524.
13. Liu, W.H., Liu, H.B., Gao, D.K., Ge, G.Q., Zhang, P., Sun, S.R., Wang, H.M., and Liu, S.B. (2013). ABCG2 protects kidney side population cells from hypoxia/reoxygenation injury through activation of the MEK/ERK pathway. *Cell Transplant.* 22, 1859–1868.
14. Pawson, T. (2002). Regulation and targets of receptor tyrosine kinases. *Eur. J. Cancer* 38 (Suppl 5), S3–S10.
15. Shukla, S., Robey, R.W., Bates, S.E., and Ambudkar, S.V. (2009). Sunitinib (Sutent, SU11248), a small-molecule receptor tyrosine kinase inhibitor, blocks function of the ATP-binding cassette (ABC) transporters P-glycoprotein (ABCB1) and ABCG2. *Drug Metab. Dispos.* 37, 359–365.
16. D’Cunha, R., Bae, S., Murry, D.J., and An, G. (2016). TKI combination therapy: strategy to enhance dasatinib uptake by inhibiting Pgp- and BCRP-mediated efflux. *Biopharm. Drug Dispos.* 37, 397–408.
17. Zhang, G.N., Zhang, Y.K., Wang, Y.J., Gupta, P., Ashby, C.R., Jr., Alqahtani, S., Deng, T., Bates, S.E., Kaddoumi, A., Wurlpel, J.N.D., et al. (2018). Epidermal growth factor receptor (EGFR) inhibitor PD153035 reverses ABCG2-mediated multidrug resistance in non-small cell lung cancer: in vitro and in vivo. *Cancer Lett.* 424, 19–29.
18. Zhang, G.N., Zhang, Y.K., Wang, Y.J., Barbuti, A.M., Zhu, X.J., Yu, X.Y., Wen, A.W., Wurlpel, J.N.D., and Chen, Z.S. (2017). Modulating the function of ATP-binding cassette subfamily G member 2 (ABCG2) with inhibitor cabozantinib. *Pharmacol. Res.* 119, 89–98.
19. Jackson, T.L., Boyer, D., Brown, D.M., Chaudhry, N., Elman, M., Liang, C., O’Shaughnessy, D., Parsons, E.C., Patel, S., Slakter, J.S., and Rosenfeld, P.J. (2017). Oral tyrosine kinase inhibitor for neovascular age-related macular degeneration: a phase 1 dose-escalation study. *JAMA Ophthalmol.* 135, 761–767.
20. Pecun, P.E., and Kaiser, P.K. (2015). Current phase 1/2 research for neovascular age-related macular degeneration. *Curr. Opin. Ophthalmol.* 26, 188–193.
21. Yan, X., Sheng, X., Tang, B., Chi, Z., Cui, C., Si, L., Mao, L.L., Lian, B., Li, S., and Zhou, L. (2017). Anti-VEGFR, PDGFR, and CSF1R tyrosine kinase inhibitor CM082 (X-82) in combination with everolimus for treatment of metastatic renal cell carcinoma: a phase 1 clinical trial. *Lancet Oncol.* 18 (Suppl 8), [https://doi.org/10.1016/S1470-2045\(17\)30764-7](https://doi.org/10.1016/S1470-2045(17)30764-7).
22. Robey, R.W., Honjo, Y., Morisaki, K., Nadjem, T.A., Runge, S., Risbood, M., Poruchynsky, M.S., and Bates, S.E. (2003). Mutations at amino-acid 482 in the ABCG2 gene affect substrate and antagonist specificity. *Br. J. Cancer* 89, 1971–1978.
23. Shi, Z., Parmar, S., Peng, X.X., Shen, T., Robey, R.W., Bates, S.E., Fu, L.W., Shao, Y., Chen, Y.M., Zang, F., and Chen, Z.S. (2009). The epidermal growth factor tyrosine kinase inhibitor AG1478 and erlotinib reverse ABCG2-mediated drug resistance. *Oncol. Rep.* 21, 483–489.
24. Dey, A., Wong, E., Kua, N., Teo, H.L., Tergaonkar, V., and Lane, D. (2008). Hexamethylene bisacetamide (HMBA) simultaneously targets AKT and MAPK pathway and represses NFκB activity: implications for cancer therapy. *Cell Cycle* 7, 3759–3767.
25. Oh, S.Y., Song, J.H., Gil, J.E., Kim, J.H., Yeom, Y.I., and Moon, E.Y. (2006). ERK activation by thymosin-beta-4 (TB4) overexpression induces paclitaxel-resistance. *Exp. Cell Res.* 312, 1651–1657.
26. Wu, S., and Fu, L. (2018). Tyrosine kinase inhibitors enhanced the efficacy of conventional chemotherapeutic agent in multidrug resistant cancer cells. *Mol. Cancer* 17, 25.
27. Dai, C.L., Liang, Y.J., Wang, Y.S., Tiwari, A.K., Yan, Y.Y., Wang, F., Chen, Z.S., Tong, X.Z., and Fu, L.W. (2009). Sensitization of ABCG2-overexpressing cells to conventional chemotherapeutic agent by sunitinib was associated with inhibiting the function of ABCG2. *Cancer Lett.* 279, 74–83.
28. Chen, L.M., Wu, X.P., Ruan, J.W., Liang, Y.J., Ding, Y., Shi, Z., Wang, X.W., Gu, L.Q., and Fu, L.W. (2004). Screening novel, potent multidrug-resistant modulators from imidazole derivatives. *Oncol. Res.* 14, 355–362.
29. Shi, Z., Liang, Y.J., Chen, Z.S., Wang, X.W., Wang, X.H., Ding, Y., Chen, L.M., Yang, X.P., and Fu, L.W. (2006). Reversal of MDR1/P-glycoprotein-mediated multidrug resistance by vector-based RNA interference in vitro and in vivo. *Cancer Biol. Ther.* 5, 39–47.
30. Zhang, W., Chen, Z., Chen, L., Wang, F., Li, F., Wang, X., and Fu, L. (2017). ABCG2-overexpressing H460/MX20 cell xenografts in athymic nude mice maintained original biochemical and cytological characteristics. *Sci. Rep.* 7, 40064.
31. Rabindran, S.K., Ross, D.D., Doyle, L.A., Yang, W., and Greenberger, L.M. (2000). Fumitremorgin C reverses multidrug resistance in cells transfected with the breast cancer resistance protein. *Cancer Res.* 60, 47–50.
32. Ambudkar, S.V. (1998). Drug-stimulatable ATPase activity in crude membranes of human *MDR1*-transfected mammalian cells. *Methods Enzymol.* 292, 504–514.
33. Dai, C.L., Tiwari, A.K., Wu, C.P., Su, X.D., Wang, S.R., Liu, D.G., Ashby, C.R., Jr., Huang, Y., Robey, R.W., Liang, Y.J., et al. (2008). Lapatinib (Tykerb, GW572016) reverses multidrug resistance in cancer cells by inhibiting the activity of ATP-binding cassette subfamily B member 1 and G member 2. *Cancer Res.* 68, 7905–7914.
34. Shukla, S., Robey, R.W., Bates, S.E., and Ambudkar, S.V. (2006). The calcium channel blockers, 1,4-dihydropyridines, are substrates of the multidrug resistance-linked ABC drug transporter, ABCG2. *Biochemistry* 45, 8940–8951.
35. Livak, K.J., and Schmittgen, T.D. (2001). Analysis of relative gene expression data using real-time quantitative PCR and the 2(−ΔΔC(T)) method. *Methods* 25, 402–408.